

The influence of growth hormone/insulin-like growth factor deficiency on prostatic dysplasia in pbARR2-Cre, PTEN knockout mice

K Takahara^{1,2,6}, N Ibuki^{1,6}, M Ghaffari^{1,3}, H Tearle¹, CJ Ong¹, H Azuma², ME Gleave^{1,4}, M Pollak⁵ and ME Cox^{1,4}

BACKGROUND: Elevated insulin-like growth factor-I (IGF-I) serum levels and phosphatase and tensin homolog (PTEN) loss are prostate cancer (PCa) risk factors that enhance androgen-responsive and castration-resistant PCa xenografts growth.

METHODS: The impact of suppressed growth hormone (GH)/IGF-I levels on neoplastic initiation of PTEN-deficient prostate epithelia was assessed histologically and by epithelial-to-mesenchymal marker expression in Ghrhr D60G homozygous (*lit/lit*) and heterozygous (*lit/+*) pbARR2-Cre, PTEN(f/f) (PTEN $-/-$) mice. How suppressed GH/IGF-I levels impacted growth of PTEN $-/-$ mouse-derived prostate cells (MPPK) was examined by growth and survival signaling of cells cultured in *lit/+* or *lit/lit* serum.

RESULTS: Body weight, prostate weight and serum GH and IGF-I levels were reduced in *lit/lit* relative to *lit/+* PTEN $-/-$ littermates. While the anterior lobes of *lit/+* PTEN $-/-$ prostates consistently presented swollen, indicative of ductal blockage, the degree of prostatic dysplasia in 15- and 20-week-old *lit/lit* and *lit/+* PTEN $-/-$ mice was indistinguishable as measured by normalized prostatic weight, tissue histology, or probasin, PSP94, E-cadherin, N-cadherin and vimentin expression. However, growth and AKT activation of MPPK cells was decreased when cultured in *lit/lit* serum as compared with *lit/+* serum and restored in *lit/lit* serum supplemented with IGF-I and, to a lesser extent, GH.

CONCLUSIONS: These results suggest that initiation of prostate carcinogenesis by loss of PTEN is not influenced by germline variation of genes encoding signaling molecules in the GH/IGF-I axis, but suggests that these factors may affect the progression of dysplastic phenotype and supports previous studies, indicating that the GH/IGF milieu does impact the growth of PTEN-deficient dysplastic prostatic cells once transformed.

Keywords: prostatic intraepithelial neoplasia; transgenic mouse; endocrine hormone; phosphatase tensin homolog; growth hormone receptor hormone

INTRODUCTION

The growth hormone and insulin-like growth factor-I (GH/IGF-I) axis is an important regulator of growth, survival and metastatic potential in a variety of malignancies and is strongly implicated in prostate cancer (PCa) etiology and risk.^{1–4} Perturbations in intrinsic expression of IGF axis components by tumor cells are implicated in susceptibility and progression of PCa.^{5–12} IGF-I receptor (IGF-1R) expression is elevated in metastatic PCa^{13,14} and castration-resistant disease progression is associated with increased expression of IGF-I and IGF-1R.¹⁵ Furthermore, maintaining IGF-I responsiveness facilitates PCa survival and growth, and is achieved through androgen-modulated IGF-1R expression.^{14,16,17}

IGF-I is a potent mitogen and antiapoptotic factor predominantly produced by the liver in response to GH signaling.¹⁸ Ligand activation of IGF-1R results in the activation of multiple intracellular signaling pathways, including RAS/extracellular signal-regulated kinases (ERKs) 1 and 2 and phosphatidylinositol-3 kinase (PI3K)/AKT that control the various IGF-mediated biological

effects.¹⁹ Activating mutations of PI3K have also been linked to PCa progression,²⁰ indicating the importance of deregulated PI3K signaling in PCa. The phosphatidylinositol phosphatase tumor suppressor, PTEN, is an important negative regulator of PI3K signaling. Homozygous loss of PTEN is a recurrent event in advanced PCa,²¹ and among those patients who are not PTEN null, many exhibit loss of one PTEN allele.²² We have previously reported that the GH/IGF-I axis is important for androgen-responsive growth, castration-resistant progression and growth of androgen receptor (AR)-negative, PTEN-deficient PCa xenografts in the *lit/lit* GH-releasing hormone-R loss-of-function murine host.²³ In addition, hemizygous PTEN loss, alone and in combination with the presence of TMPRSS2-ERG gene rearrangements, are reported in early stages of disease and to predict an increased risk of biochemical progression.^{24,25} This prediction is supported by the demonstration that a murine model for prostate-conditional PTEN loss is sufficient to induce development²⁶ and castration-resistant progression²⁷ of PCa. These results indicate that PTEN

¹The Vancouver Prostate Centre, Vancouver General Hospital, Vancouver, British Columbia, Canada; ²Department of Urology, Osaka Medical College, Osaka, Japan; ³Department of Medicine, University of British Columbia, Vancouver, British Columbia, Canada; ⁴Department of Urologic Sciences, University of British Columbia, Vancouver, British Columbia, Canada and ⁵Department of Medicine and Oncology, McGill University, Montreal, Quebec, Canada. Correspondence: Dr ME Cox, The Vancouver Prostate Centre, Vancouver General Hospital, 2660 Oak Street, Vancouver, British Columbia, Canada V6H 3Z6.

E-mail: mcox@prostatecentre.com

⁶These authors contributed equally to this work.

loss can hypersensitize cells to PI3K activation by factors such as GH and IGF-I.

To test the hypothesis that dysplastic initiation of PTEN-deficient prostate epithelial cells may be due to hypersensitivity to GH/IGF-mediated PI3K signaling, we assessed development of prostatic dysplasia in *Ghrhr* D60G (*lit*) × *pbARR2-Cre*, *PTEN*(*fl/fl*) mice (*PTEN* −/−). Our *in vivo* and *in vitro* results suggest that prostatic dysplasia induced by *PTEN* loss is not substantially affected by *Ghrhr* deficiency, but subsequent growth of dysplastic epithelia is impaired in hosts carrying germline deficiencies for GH and IGF-I expression, and may affect the progression of dysplastic phenotype in PCa.

MATERIALS AND METHODS

Ghrhr(*lit/lit*) and (*lit*/+) *pbARR2-Cre*/*PTEN*(*fl/fl*) mouse characterization

PTEN(*fl/fl*) C57BL/6J mice were obtained from T. Mak (Toronto, Canada)²⁸ *pbARR2-Cre* created in a C57BL/6 × DBA2 hybrid mouse strain was obtained from P. Roy-Berman (Los Angeles, CA)²⁹ and *Ghrhr* D60G (*lit/lit*) C57BL/6J mice were from Jackson Laboratory (Bar Harbor, ME).³⁰ *pbARR2-Cre*, *PTEN*(*fl/fl*) mice (*PTEN* −/−) generated, as described previously,³¹ were crossed with *lit/lit* mice to produce *lit/lit* and *lit*/+ *PTEN* −/− mice. This transgenic strain was genotyped to confirm the status of the *Ghrhr* allele mutation as described previously,²³ as well as confirming *Cre* recombinase and *PTEN*(*fl/fl*) status from tail clip DNA extracted using DirectPCR Lysis Reagent (Viagen Biotech, Los Angeles, CA, USA) and maintained by backcrossing. The extent of prostatic dysplasia was assessed in *lit/lit* and *lit*/+ *PTEN* −/− mice at 15 and 20 weeks of age (10 mice per cohort). Prostate weights were determined after dissection and lancing of the *lit*/+ anterior lobes to remove retained fluid. Prostate pathology was scored from formalin-fixed, paraffin-embedded, hematoxylin- and eosin-stained specimens by a blinded pathologist (L Fazli). Probasin, PSP94, E-cadherin, N-cadherin and vimentin transcript levels were measured from total RNA prepared from flash-frozen total prostates by quantitative real-time polymerase chain reaction normalized to murine β -actin transcript for each specimen. Male mice were harvested in accordance with the guidelines of the Canadian Council on Animal Care and with appropriate institutional certification.

Cell lines

MPPK cells were established from prostate tissue from a 40-week-old *pbARR2-Cre*, *PTEN*(*fl/fl*) male mice as described³¹ and maintained in Dulbecco's modified Eagle's medium supplemented with 10% fetal bovine serum. LNCaP cells (courtesy of Dr LWK Chung, City of Hope Hospital, Los Angeles, CA, USA) were maintained in RPMI1640 + 5% fetal bovine serum and DU145 cells purchased from American Type Culture Collection (Rockville, MD, USA) were maintained in Dulbecco's modified Eagle's medium + 5% fetal bovine serum. Cells were cultured at 37 °C in a humidified 5% CO₂ atmosphere with media supplies purchased from Life Technologies (Burlington, Ontario, Canada).

In vitro cell proliferation assay

MPPK cells were cultured in *lit/lit* and *lit*/+ serum and in *lit/lit* serum supplemented with recombinant murine GH (R&D Systems, Minneapolis, MN, USA) or IGF-I (Calbiochem, San Diego, CA, USA) at the indicated concentrations. Proliferation was measured by pulse-labeling cells for 2 h with 10 μ M bromodeoxyuridine (BrdU) after 46 h in culture. Denatured DNA in fixed cells was stained with a peroxidase-coupled anti-BrdU-antibody and peroxidase substrate (tetramethylbenzidine) for 30 min and BrdU incorporation was measured by densitometry (OD 370 nm). Each assay was performed in triplicate.

Immunoblot analysis

Whole-cell protein lysates of LNCaP, DU145 and MPPK cells cultured in serum-free RPMI-1640 for 2 days \pm 1 nM methyltrienolone, a synthetic androgen (R1881; Perkin-Elmer, Waltham MA, USA), were prepared in RIPA buffer (50 mM Tris-HCl, pH 7.2, 1% NP-40, 0.1% deoxycholate, 0.1% sodium dodecyl sulfate, 100 mM NaCl, 1 × Roche complete protease inhibitor cocktail), subjected to sodium dodecyl sulfate-polyacrylamide gel electrophoresis and transferred to nitrocellulose filters for immunoblotting with

primary antibody (Ab): anti-AR and anti-vimentin rabbit polyclonal Ab (Santa Cruz Biotechnology, Santa Cruz, CA, USA), anti-PTEN rabbit polyclonal Ab (Cell Signaling Technology, Danvers, MA, USA), anti-E-cadherin and anti-N-cadherin mouse monoclonal Ab (BD Biosciences, San Jose, CA, USA) and anti- β -actin mouse monoclonal Ab (Millipore Corporation, Billerica, MA, USA). Immunoreactive proteins were detected by enhanced chemiluminescence western blotting analysis system (Amersham Life Science, Arlington Heights, IL, USA), using horseradish peroxidase-conjugated anti-rabbit or anti-mouse IgG Ab (Santa Cruz).

Whole-cell lysates of MPPK cells cultured in media supplemented with 1% *lit/lit* or 1% *lit*/+ mouse serum for 2 days, or cultured 24 h in serum-free media, washed and then stimulated with media containing 1% *lit/lit* serum containing the indicated concentrations of recombinant murine GH or IGF-I for 20 min were immunoblotted with anti-vinculin mouse monoclonal Ab (Sigma Chemical, St Louis, MO, USA), anti-phospho-AKT (S473) rabbit polyclonal Ab, anti-AKT rabbit polyclonal Ab, anti-phospho-ERK1/2 (T185/Y187 and T202/Y204, respectively) rabbit polyclonal Ab, anti-ERK1/2 rabbit polyclonal Ab (all from Cell Signaling Technology) and detected by enhanced chemiluminescent as above.

Statistical analysis

Data were analyzed by analysis of variance and Mann-Whitney *post hoc* test, except for paired tests that were analyzed by Student's *t*-test. Levels of statistical significance were set at $P < 0.05$.

RESULTS

lit/lit *PTEN* −/− mice and *lit*/+ *PTEN* −/− mice display extensive prostatic dysplasia

To compare the impact of GH/IGF-I axis deficiency on development of prostatic dysplasia induced by loss of *PTEN* in the murine prostate, 10 *lit/lit* and *lit*/+ *PTEN* −/− mice were collected at 15 and 20 weeks of age. Macroscopic examination of the prostates from *lit/lit* *PTEN* −/− and *lit*/+ *PTEN* −/− mice revealed overtly hypertrophic anterior prostate lobes in both cohorts (Figures 1a and b, respectively). However, the anterior prostate lobes from *lit*/+ *PTEN* −/− mice consistently presented as swollen and fluid-filled, while those from *lit/lit* *PTEN* −/− mice were enlarged and structurally nodular, with no evidence of fluid retention. Histopathologic analysis of dysplastic prostates from *lit/lit* and *lit*/+ *PTEN* −/− mice (Figures 1c and d, respectively) revealed that both cohorts exhibited uniformly mild-to-severe epithelial dysplasia in the anterior, ventral and dorsolateral prostatic lobes, with no clear evidence of stromal invasion, consistent with induction of prostatic intraepithelial neoplasia as previously reported in *PTEN* −/− mice.³²

As predicted from the known effects of the *Ghrhr* D60G deficiency of *lit/lit* mice, the average serum GH level of *lit/lit* *PTEN* −/− mice at 15 and 20 weeks (0.2 and 0.6 ng ml^{−1}, respectively) was on average ~1/10th that measured in *lit*/+ *PTEN* −/− mice (3.1 and 3.5 ng ml^{−1}, respectively; Figure 2a). Correspondingly, the average serum IGF-I level of *lit/lit* mice at 15 and 20 weeks (37 and 42 ng ml^{−1}, respectively) was ~1/6th that measured in *lit*/+ *PTEN* −/− littermates (247 and 267 ng ml^{−1}; Figure 2b). Consistent with our previous characterizations of male *lit/lit* and *lit*/+ mice,²³ the average body weight of *lit/lit* *PTEN* −/− mice (18 and 20 g at 15 and 20 weeks, respectively) was ~60% that of the *lit*/+ *PTEN* −/− littermates (31 and 33 g at 15 and 20 weeks, respectively) (Figure 2c). To normalize tissue weights, the anterior prostate lobes of the *lit*/+ *PTEN* −/− mice were drained of retained fluid. The resulting lanced weight of the prostates from *lit/lit* *PTEN* −/− mice at 15 and 20 weeks (0.13 and 0.17 g, respectively) were also proportionally smaller (~60%) than that of their *lit*/+ littermates (0.19 and 0.25 g, respectively; Figure 2d). We next assessed whether *PTEN* −/− prostatic dysplasia was distinguishable when normalized for intrinsic differences in body size of *lit/lit* and *lit*/+ mice, the prostate:body weight ratio was calculated for each animal and the average body weight-normalized prostate weight ratio was compared between

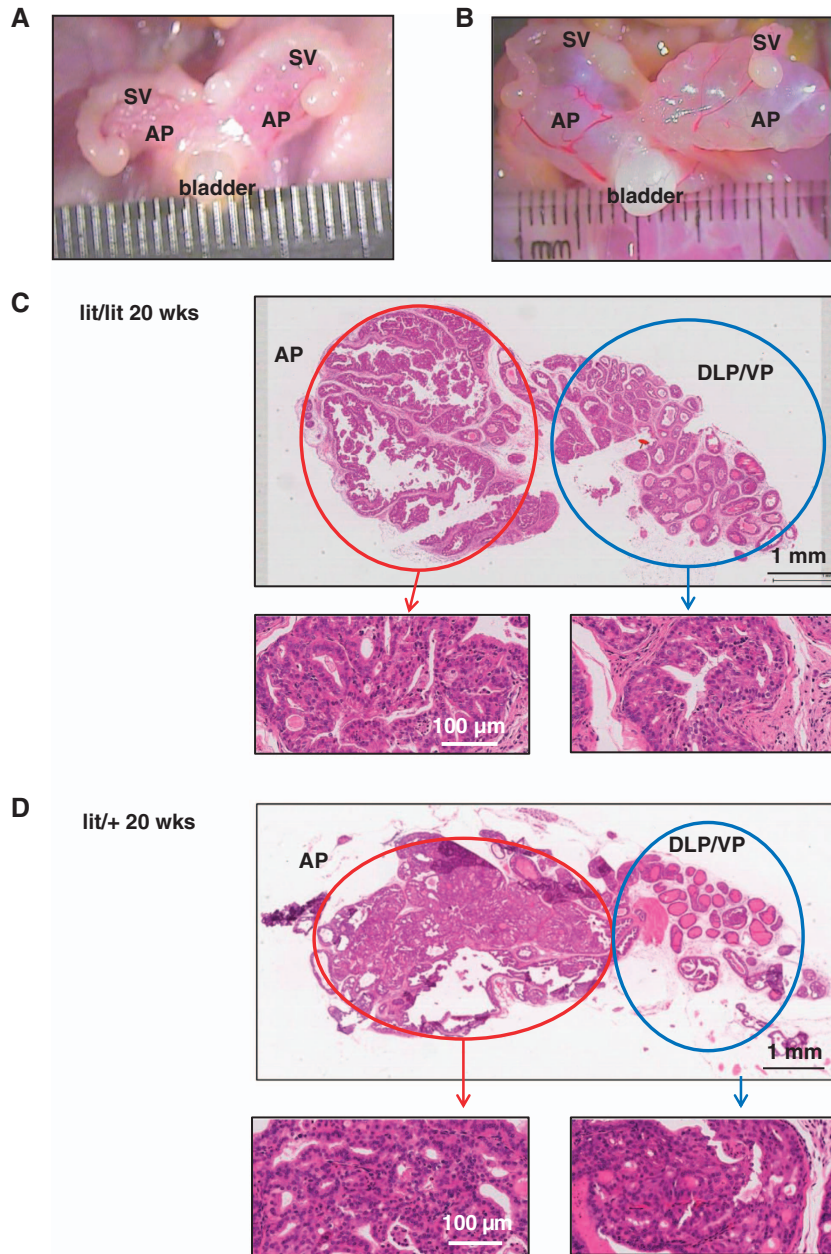


Figure 1. *lit/lit* PTEN^{-/-} and *lit/+* PTEN^{-/-} mice display extensive prostatic dysplasia. Representative macroscopic images of (a) *lit/lit* PTEN^{-/-} mouse and (b) *lit/+* PTEN^{-/-} mouse prostates show overtly hypertrophic anterior prostate (AP) below seminal vesicles (SV) and urinary bladder. Representative low magnification (upper panels, scale bar = 1 mm) and high magnification (lower panels, scale bar = 100 μm) microscopic images of hematoxylin- and eosin-stained sections of dysplastic mouse AP, dorsal-lateral prostate (DLP) and ventral prostate (VP) from (c) *lit/lit* PTEN^{-/-} 20 weeks and (d) *lit/+* PTEN^{-/-} 20 weeks. PTEN, phosphatase and tensin homolog.

the *lit/lit* and *lit/+* PTEN^{-/-} cohorts (Figure 2e). Again, the body weight-normalized prostate weight ratio was indistinguishable between the PTEN^{-/-} *lit/lit* and *lit/+* cohorts at 15 or 20 weeks; however, there was a significant increase in the prostate weight increase from 15 to 20 weeks for the *lit/+* cohort (60 mg) but not in the *lit/lit* cohort (30 mg).

Furthermore, immunohistochemical analysis for Ki-67 staining of the dysplastic prostatic epithelia revealed that the mitotic activity between cohorts was indistinguishable (Supplementary Figure S1). Specimens were also assessed for PI3K activity as measured by phospho S473-Akt (pAKT) immunohistochemical staining intensity normalized to AR positivity as a marker of epithelial cell density (Supplementary Figure S2). While we

observed high constitutive pAKT levels, as expected, from prostatic PTEN knockout, there was no measurable difference in pAKT levels between cohorts.^{26,32} We conclude that elevated basal PI3K signaling and mitotic activity in PTEN-deficient prostates does not require normal physiologic IGF-I or GH levels.

In a parallel analysis, we compared prostatic pathology of 15-week-old *lit/lit* PTEN^{-/-} mice with Ghrhr wild-type (wt) PTEN^{-/-} mice (Supplementary Figure S3). The overtly hypertrophic and swollen prostatic phenotype of the Ghrhr wt PTEN^{-/-} mice was indistinguishable from that of age-matched *lit/+* PTEN^{-/-} mice. The body weight-normalized total prostate weights of the Ghrhr wt PTEN^{-/-} mice was 1.5 times greater than that of *lit/lit* PTEN^{-/-} mice, but again this difference was

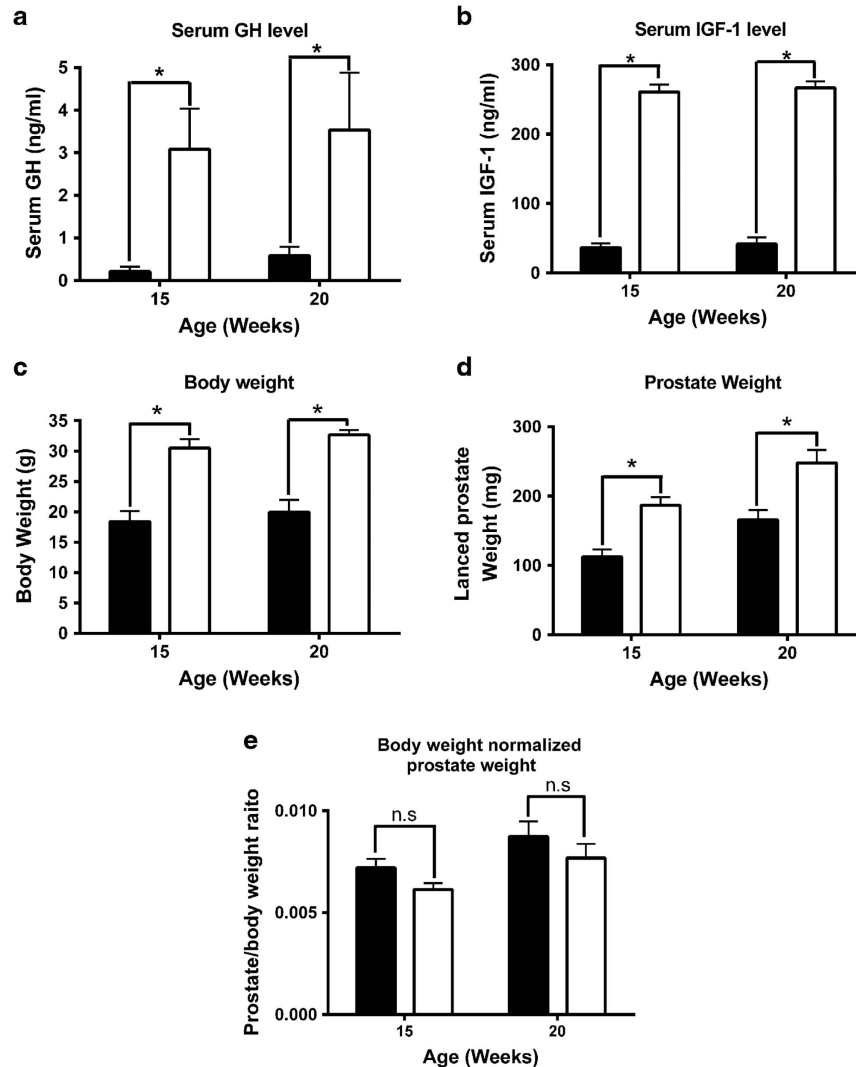


Figure 2. Comparison of *lit/lit* and *lit/+* *PTEN*^{-/-} male mouse body weight, serum growth hormone (GH) levels and serum insulin-like growth factor-1 (IGF-1) levels. Average (\pm s.e.m.) serum GH (a) and IGF-1 (b) levels, and body weight (c) and lanced prostate weight (d) of *lit/lit* (black bars) and *lit/+* (white bars) *PTEN*^{-/-} mice at 15 and 20 weeks of age. (e) Prostate:body weight ratio was calculated for each animal and the average prostate/body weight ratio (\pm s.e.m.) was plotted for *lit/lit* (black bars) and *lit/+* (white bars) *PTEN*^{-/-} mice. * $P < 0.05$ by analysis of variance and Mann-Whitney *post hoc* test; n.s., no significant difference observed for indicated comparisons. *PTEN*, phosphatase and tensin homolog.

not seen when the *Ghrhr* wt *PTEN*^{-/-} prostates were lanced to drain retained fluid. These results indicate that the lack of a difference between the *lit/lit* and *lit/+* prostate pathology was not due to a suppressed effect in response to *Ghrhr* D60G heterozygosity.

Assessment of epithelial and mesenchymal characteristics in dysplastic prostates of *lit/lit* and *lit/+* *PTEN*^{-/-} mice

To assess whether GH/IGF-1 deficiency impacts prostatic epithelial differentiation in *PTEN*^{-/-} mice, transcript levels of probasin (Figure 3a) and PSP94 (Figure 3b) were measured by real-time reverse transcription-polymerase chain reaction analysis from total RNA of each mouse prostate collected at 15 and 20 weeks of age. Although the average mean expression of these markers in the *lit/lit* cohort at 20 weeks trended higher than the average of the other three cohorts, the expression of these prostatic epithelial markers was statistically indistinguishable between the *lit/lit* and *lit/+* cohorts at either time point or between time points for each cohort.

RAS/ERK pathway activation has been reported to promote epithelial-to-mesenchymal transition (EMT) in the prostates of *PTEN*^{-/-} mice.³³ To assess whether the slightly lower average probasin and PSP94 expression in the 20-week *lit/+* cohort was associated with any evidence of EMT, real-time polymerase chain reaction was used to measure transcript levels of E-cadherin (Figure 3c), vimentin (Figure 3d) and N-cadherin (Figure 3e) from total RNA of each mouse prostate collected above. Normalized E-cadherin expression level was indistinguishable between the cohorts at either time point; however, there was an apparent increase in the relative expression of vimentin and N-cadherin transcripts from 15 to 20 weeks in both the *lit/lit* and *lit/+* cohorts. Although prostatic N-cadherin levels appeared to increase between 15 and 20 weeks in *lit/+* *PTEN*^{-/-} mice compared with the *lit/lit* *PTEN*^{-/-} mice, this difference was dominated by an apparent suppression of N-cadherin expression in the *lit/+* cohort that is likely a sampling artifact, as the mean N-cadherin expression level of the 15-week *lit/lit* and *lit/+* *PTEN*^{-/-} cohorts was statistically indistinguishable. However, when protein expression for these markers was assessed from

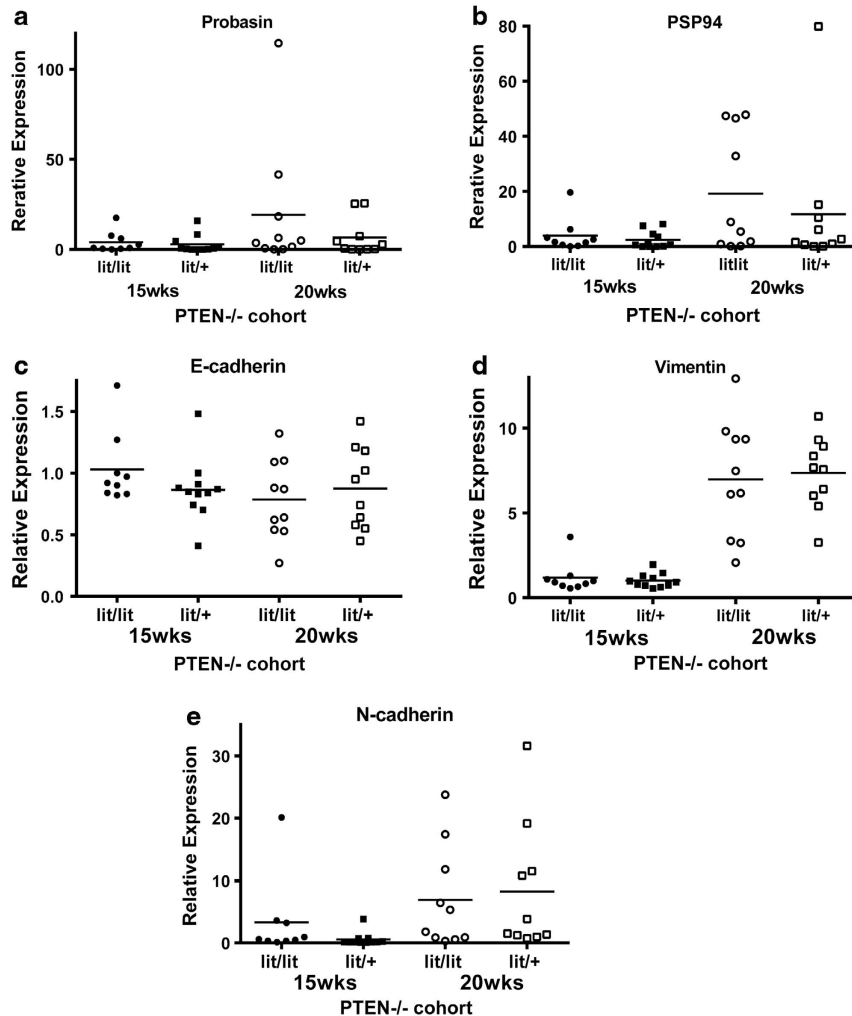


Figure 3. Expression of prostatic differentiation markers and evidence of EMT in $PTEN^{-/-}$ *lit/lit* and *lit/+* mice. Real-time reverse transcription-polymerase chain reaction was used to analyze probasin (a) and PSP94 (b) E-cadherin (c), vimentin (d) and N-cadherin (e) mRNA from total prostate RNA collected at 15 and 20 weeks of age. Scatter plots represent relative mRNA level for each mouse prostate sample. Circles = *lit/lit* animals, squares = *lit/+* animals, black = 15 week old animals and white = 20 week old animals. Bar designates mean relative expression of respective mRNAs for each $PTEN^{-/-}$ cohort. EMT, epithelial-to-mesenchymal transition; PTEN, phosphatase and tensin homolog.

prostatic lysates by immunoblotting normalized to β -actin levels, these trends for increased vimentin and N-cadherin expression in the 20-week cohorts were not confirmed (Supplementary Figure S4).

We conclude that although the consistently observed swelling of the anterior prostate lobes in the *lit/+* $PTEN^{-/-}$ mouse, indicative of blocked terminal prostatic ducts in these animals, suggests that dysplastic progression is delayed in the *lit/lit* hosts, morphologic and molecular marker expression changes indicate that genomic alterations that result in suppressed GH/IGF-I axis signaling do not affect initiation of prostatic dysplasia because of PTEN deletion.

Characterization of EMT marker expression in MPPK cells

We next assessed whether the previously established $PTEN^{-/-}$ mouse prostate cell line, MPPK, harbored any of the EMT characteristics implicated above by characterizing them for expression of prostatic epithelial and mesenchymal markers relative to that observed in well-characterized, androgen-responsive human prostate cancer cell line, LNCaP, and androgen-independent, AR-negative human prostate cancer cell line, DU145 (Figure 4a). MPPK cells expressed AR and this expression was

enhanced in the presence of R1881. Androgen responsiveness was confirmed by firefly luciferase reporter assay in MPPK cells transfected with pbARR2-Luc and stimulated 24h with R1881 (Figure 4b). MPPK cells were also confirmed to be deficient for PTEN expression by comparison to expression in the $PTEN$ wt DU145 cells and the $PTEN$ -null LNCaP cells. MPPK cells exhibited robust E-cadherin expression, comparable to that observed in LNCaP cells. While MPPK cells expressed vimentin at low levels, comparable to that of LNCaP cells, relative to the robust expression in DU145 cells, they did express high levels of N-cadherin not observed in LNCaP and DU145 cells. This observation is consistent with the suggestion that $PTEN^{-/-}$ prostatic epithelial cells acquire intermediary mesenchymal characteristics while still in an intraepithelial neoplastic state and indicate that the MPPK cell line accurately reflects the phenotype of the dysplastic prostatic epithelia of $PTEN^{-/-}$ cells.

Growth of MPPK cells is suppressed in media supplemented with *lit/lit* serum

To determine if growth characteristics of MPPK cells were sensitive to changes in GH/IGF-I levels, relative proliferation of MPPK cells cultured in basal media + 1% *lit/lit* serum or 1% *lit/+* serum was

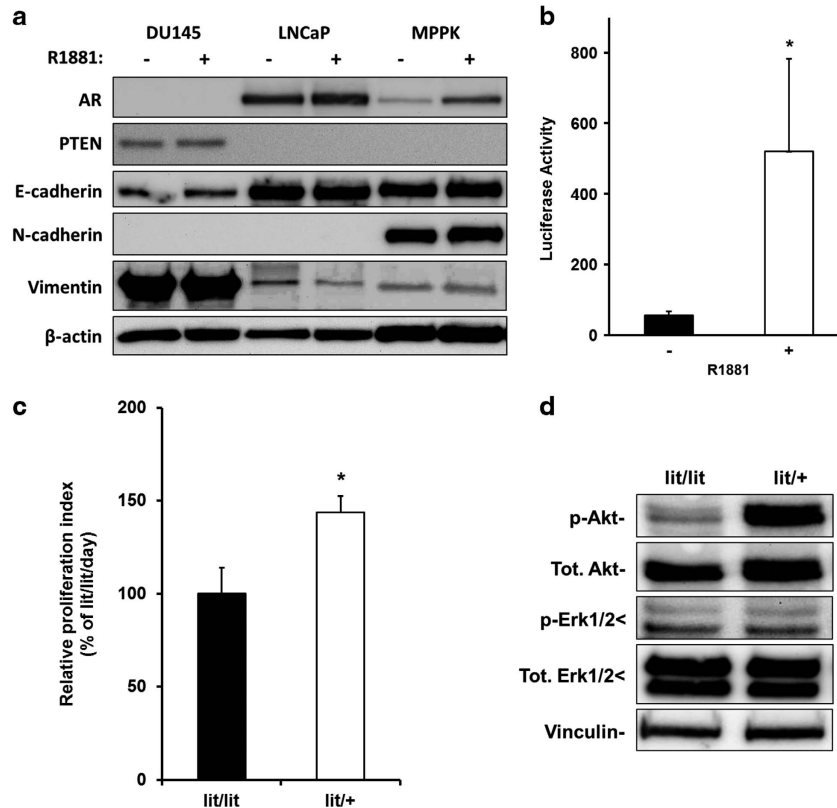


Figure 4. Epithelial and mesenchymal characteristics of mouse-derived prostate (MPPK) cells. (a) Immunoblot analysis of prostatic epithelial and mesenchymal marker expression in MPPK cells relative to that observed in LNCaP and DU145 PCa cells. Cells were cultured in serum-free media for 2 days \pm 1 nM R1881 were immunoblotted for androgen receptor (AR), PTEN, E-cadherin, N-cadherin, vimentin and β -actin expression. (b) Androgen responsiveness of MPPK cells assessed by firefly luciferase reporter activity of cells transfected with pbARR2-Luc \pm stimulation 24 h with 1 nM R1881. (c) Relative proliferation was examined in MPPK cells cultured in basal media + 1% *lit/lit* serum (black bar) or 1% *lit/+* serum (white bar) for 2 days by BrdU incorporation. Data are expressed as fold-change in proliferation in *lit/+* serum normalized to that in *lit/lit* serum at each day (mean \pm s.d., $n = 3$, * $P < 0.05$ by Student's *t*-test). (d) Immunoblots of whole-cell lysates of MPPK cells collected after culture in 1% *lit/lit* serum or 1% *lit/+* serum for 2 days for p-AKT, t-AKT, p-ERK1/2, t-ERK1/2 and vinculin expression. Immunoblots in (a) and (d) are representative of three independent experiments. PTEN, phosphatase and tensin homolog.

examined by BrdU incorporation (Figure 4c). Mitotic activity of MPPK cells cultured in 1% *lit/+* serum was significantly elevated (~40%) relative to that of cells cultured in 1% *lit/lit* serum. RAS/mitogen-activated protein kinase and PI3K/AKT signaling have been implicated in transformation of PTEN $-/-$ murine prostate epithelia. The effect of these culture conditions on steady-state RAS/mitogen-activated protein kinase and PI3K/AKT signaling was assessed by immunoblotting of MPPK, whole-cell lysates after culture in 1% *lit/lit* serum or 1% *lit/+* serum for 2 days for phospho- and total AKT and ERK, and vinculin (Figure 4d). Densitometric quantification of phospho- to total AKT and Erk revealed that steady-state phospho-AKT levels were on average elevated fivefold, while phospho-ERK levels were not affected in cells cultured in *lit/+* serum vs those cultured in *lit/lit* serum. These observations are consistent with enhanced PI3K/AKT signaling in PTEN-deficient cells when cultured in the presence of GH- and IGF-I-containing serum.

Suppressed growth of MPPK cells in *lit/lit* serum can be rescued by the addition of GH or IGF-I

To determine whether GH or IGF-I were sufficient to promote growth in *lit/lit* serum, MPPK cells were cultured in 1% *lit/lit* serum \pm recombinant GH (0.1, 1 and 10 ng ml $^{-1}$) or recombinant IGF-I (5, 50 and 100 ng ml $^{-1}$) or 1% *lit/+* serum for 2 days (Figure 5a). Relative mitotic activity was measured by BrdU incorporation and expressed relative to that of cells cultured

without the addition of exogenous growth factors. The addition of GH to levels equal to or greater than that found in *lit/+* serum marginally affected MPPK cell proliferation, while supplementing *lit/lit* serum with IGF-I significantly enhanced MPPK proliferation at all concentrations tested. In contrast, proliferation of MPPK cells cultured in GH was significantly lower than that of cells grown in *lit/+* serum, while proliferation of cells grown in IGF-I were indistinguishable from that of cells grown in *lit/+* serum. These results suggest that suppressed IGF-I levels are primarily responsible for lower proliferation rate of MPPK cells *in vitro*.

To assess if intracellular signaling pathways were altered by growth factor supplementation of the *lit/lit* serum, lysates of MPPK cells cultured 24 h in serum-free media and stimulated with 1% *lit/lit* serum plus 0, 0.1 and 1 ng ml $^{-1}$ GH, or 0, 5 and 50 ng ml $^{-1}$ IGF-I for 20 min were immunoblotted against phospho- and total AKT and ERK, and vinculin (Figure 5b). Paralleling the observed changes in cell growth, GH did not affect steady-state AKT or ERK activation at the 20 min time-point, while IGF-1 did promote AKT activation. These results are consistent with the differences observed in proliferation and AKT activation in MPPK cells cultured in *lit/lit* vs *lit/+* serum and suggests that IGF-I can rescue suppressed proliferation of these cells in serum from *lit/lit* mice.

DISCUSSION

The GH/IGF-I axis and downstream signaling pathways, such as RAS/ERK and PI3K/AKT, have established roles in PCa patho-

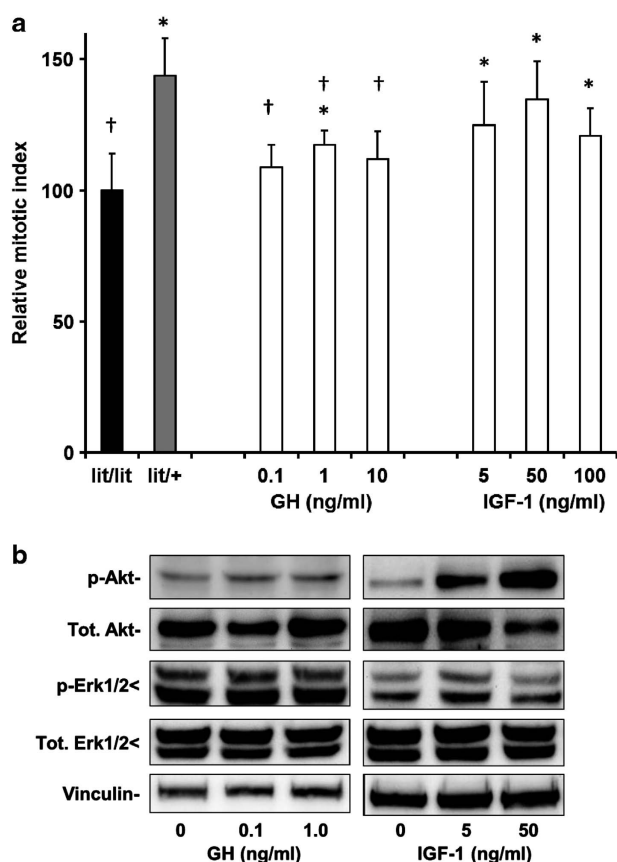


Figure 5. *In vitro* proliferation and activation of AKT and ERK1/2 signaling in MPPK cells cultured in *lit/lit* serum supplemented with recombinant growth hormone (GH) and insulin-like growth factor-1 (IGF-I). MPPK cells were cultured in 1% *lit/+* or *lit/lit* serum \pm recombinant GH (0.1, 1 and 10 ng ml⁻¹) or recombinant IGF-I (5, 50 and 100 ng ml⁻¹) serum for 2 days. (a) Relative proliferation was measured by BrdU incorporation as in Figure 4 and expressed relative to that of cells cultured in *lit/lit* serum without the addition of exogenous growth factors (black bar) (mean \pm s.d., $n=3$, * $P<0.05$) or in *lit/+* serum without exogenous growth factors (gray bar) (mean \pm s.d., $n=3$, † $P<0.05$). (b) Immunoblots of whole-cell lysates from MPPK cells cultured 24 h in serum-free media and stimulated with 1% *lit/lit* serum + 0, 0.1 and 1 ng ml⁻¹ GH, or + 0, 5 and 50 ng ml⁻¹ IGF-I for 20 min for p-AKT, t-AKT, p-ERK1/2, t-ERK1/2 and vinculin expression. Immunoblots are representative of three independent experiments. MPPK, mouse-derived prostate cells.

logy.^{14,15,19,34} In addition, IGF-I expression and signaling or host GH and IGF-I levels are important regulators of PTEN-deficient human PCa cell xenograft growth.^{23,35} Using the probasin-SV40 T-Ag (TRAMP) prostate cancer animal model, we previously observed that tumor development was delayed when crossed into the *lit/lit* background, suggesting that risk of prostate carcinogenesis and progression may be influenced by germline variation of genes encoding signaling molecules in the GH/IGF-I axis.³⁴ In contrast, development of TRAMP tumors in hosts harboring targeted deletion of hepatic IGF-I did not show a delay in prostate carcinogenic kinetics, suggesting that differences in GH levels may impact TRAMP tumorigenic potential.³⁶

To help resolve how host GH and IGF levels might impact disease initiation, we assessed the impact of GH and IGF-I deficiency on prostate cancer initiation using a model more relevant to human disease that results in perturbation in the PI3K/AKT pathway. A signature event impacting PI3K/AKT signaling in prostate cancer is hemi- and homozygous loss of the tumor suppressor, PTEN^{22,24} and prostate-specific deletion of the murine

PTEN tumor suppressor gene leads to the development of prostate cancer.²⁶ To investigate the role of GH/IGF-I axis on the initiation of neoplastic progression of prostatic epithelial cells depleted for PTEN, we crossed *lit/lit* mice with PTEN^{-/-} mice to produce *lit/lit* and *lit/+* PTEN^{-/-} mice that were analyzed for the degree of prostatic pathology of *lit/lit* and *lit/+* PTEN^{-/-} mice at 15 and 20 weeks of age. Prostates from *lit/lit* and *lit/+* PTEN^{-/-} mice exhibited elevated pAKT levels and Ki-67-positive index in the AR-positive prostatic epithelium of both PTEN^{-/-} cohorts is consistent with the loss of PTEN implicated to drive pathology in this animal model.^{26,32} While these prostates did not exhibit signs of true carcinogenic progression at the time points chosen, they did consistently display evidence of extensive prostatic dysplasia analogous to high-grade prostatic intraepithelial neoplasia. This lack of carcinogenic progression did not appear to be due to PTEN hemizyosity as Ghrhr wt PTEN^{-/-} prostates revealed dysplasia indistinguishable from that of the *lit/+* PTEN^{-/-} littermates. These observations are consistent with the kinetics of prostatic lesion formation in mice in which PTEN excision was induced at the beginning of puberty.³²

While this PTEN^{-/-} phenotype was muted relative to that reported previously,²⁶ the consistent presentation of extensive intraepithelial neoplasia still allowed for comparison of how genetic variation for GH and IGF-I expression might affect initiation of prostatic intraepithelial neoplasia due to PTEN loss. The most obvious difference in prostate pathology between the *lit/lit* and *lit/+* PTEN^{-/-} mice was the profound swelling of the anterior prostates of the *lit/+* littermates. Indeed, the increased body weight-normalized whole prostate weights of Ghrhr wt PTEN^{-/-} mice may represent a subtle decrease in epithelial expansion in the GH/IGF-I-deficient hosts if the retained fluid is composed of shed cellular mass. However, once drained of retained fluid, the body mass-normalized prostatic weights were indistinguishable between the cohorts. In addition, microscopic evaluation revealed indistinguishable degrees of epithelial hyperplasia in this or any of the other prostatic lobes of these mice. These observations are consistent with the results from systemic PTEN^{+/-} mice in which knockout of IRS2 did not affect initiation of prostatic dysplasia but did delay lesion progression.³⁷

This lack of overt phenotypic difference in prostatic dysplastic initiation compelled us to examine molecular features of the *lit/+* and *lit/lit* PTEN^{-/-} prostates. Recently, RAS/ERK activation was reported to cooperate with PTEN deficiency to promote EMT and metastatic behavior of prostatic progenitor cells.³³ We therefore assessed epithelial and mesenchymal characteristics of these cohorts. Murine prostatic epithelial differentiation marker expression (probasin, PSP94 and E-cadherin) were indistinguishable in *lit/lit* and *lit/+* PTEN^{-/-} mice at the two time points analyzed here. The expression of mesenchymal markers, vimentin and N-cadherin, showed no indistinguishable difference between our *lit/+* and *lit/lit* PTEN^{-/-} cohorts, but were readily detected in the prostates along with the epithelial marker, E-cadherin. While there was no apparent difference in presentation of EMT characteristics between the *lit/lit* and *lit/+* PTEN^{-/-} mice, observations here of prostates with mixed epithelial and mesenchymal characteristics indicate that loss of PTEN expression alone is sufficient to initiate acquisition of mesenchymal characteristics and that these characteristics persist in cells derived from lymph node metastasis of prostate-derived PTEN^{-/-} cells. Although prostatic dysplasia and acquisition of initial EMT characteristics induced by PTEN deficiency was not substantially affected by Ghrhr deficiency, these events may prime transformed cells for subsequent malignant progression by promoting expansion of cells with progenitor characteristics as described.³³

Ghrhr antagonists have been shown to suppress the growth of various human cancer lines as xenografts in immune-compromised mice, including inhibiting growth of PC3 and DU145 PCa

xenografts.^{38,39} We have previously demonstrated that decreased circulating GH and IGF-I were significant contributors to suppressed growth of both androgen-responsive and castration-resistant PTEN-null PCa cells,²³ and that antisense oligonucleotide suppression of IGF-1R expression suppressed growth of these androgen-responsive and castration-resistant PTEN-null PCa cells.³⁵ These studies supported the contention that decreased IGF-I availability and signaling from IGF-1R to AKT was the primary missing growth stimulatory pathway for such cells in the *lit/lit* host. Consistent with these previous results, in this study, growth of MPPK cells was suppressed in media supplemented with *lit/lit* serum as compared with *lit/+* serum, and that restoration of suppressed growth of MPPK cells in *lit/lit* serum by the addition of IGF-I and, to a lesser extent, GH was correlated with increased steady-state activation of AKT. In contrast to the results from TRAMP crosses with *lit/lit* or hepatic IGF-I knockout mice that implicated a role for GH in driving TRAMP tumorigenesis, these *in vitro* experiments and our previous studies implicate circulating IGF-I as the predominant contributor to proliferation of PCa, and that this effect is mediated primarily through PI3K/AKT activation.

CONCLUSION

Our *in vivo* and *in vitro* experiments suggest that loss of PTEN may initiate prostatic epithelial dysplasia and acquisition of mesenchymal characteristics and that IGF-I may be an important factor in sustaining proliferation of these dysplastic cells. We therefore suggest that in early stages of PCa development, suppression of GH/IGF-I axis may delay invasive PCa progression. Such treatments might be best augmented by therapies targeting factors that regulate EMT, a process mechanistically linked with stem cell signatures in PCa cells⁴⁰ and increased resistance to apoptosis, diminished senescence, escape from immune surveillance and eventual resistance to therapy.⁴¹ With the reports linking GH/IGF-I axis signaling to EMT and acquisition of stem-like properties, these results support continued effort to disrupt IGF axis signaling to control PCa progression.

CONFLICT OF INTEREST

The authors declare no conflict of interest.

ACKNOWLEDGEMENTS

We thank Virginia Yago, Darrell Trendall, Estelle Li and Mary Bowden for their excellent technical assistance. This work was supported by Terry Fox Program in Prostate Cancer Progression grant from the National Cancer Institute of Canada (no. 017007) and a CIHR Doctoral Fellowship award (to MG).

REFERENCES

- Chan JM, Stampfer MJ, Giovannucci E, Gann PH, Ma J, Wilkinson P *et al*. Plasma insulin-like growth factor-I and prostate cancer risk: a prospective study. *Science* 1998; **279**: 563–566.
- LeRoith D, Roberts Jr CT. The insulin-like growth factor system and cancer. *Cancer Lett* 2003; **195**: 127–137.
- Papatsoris AG, Karamouzis MV, Papavassiliou AG. Novel insights into the implication of the IGF-1 network in prostate cancer. *Trends Mol Med* 2005; **11**: 52–55.
- Ryan CJ, Haqq CM, Simko J, Nonaka DF, Chan JM, Weinberg V *et al*. Expression of insulin-like growth factor-1 receptor in local and metastatic prostate cancer. *Urol Oncol* 2007; **25**: 134–140.
- Pollak M. Insulin-like growth factor physiology and cancer risk. *Eur J Cancer* 2000; **36**: 1224–1228.
- DiGiovanni J, Kiguchi K, Frijhoff A, Wilker E, Bol DK, Beltran L *et al*. Deregulated expression of insulin-like growth factor 1 in prostate epithelium leads to neoplasia in transgenic mice. *Proc Natl Acad Sci USA* 2000; **97**: 3455–3460.
- Chan JM, Stampfer MJ, Ma J, Gann P, Gaziano JM, Pollak M *et al*. Insulin-like growth factor-I (IGF-I) and IGF binding protein-3 as predictors of advanced-stage prostate cancer. *J Natl Cancer Inst* 2002; **94**: 1099–1106.
- Grimberg A. Mechanisms by which IGF-I may promote cancer. *Cancer Biol Ther* 2003; **2**: 630–635.
- Hellawell GO, Turner GD, Davies DR, Poulosom R, Brewster SF, Macaulay VM. Expression of the type 1 insulin-like growth factor receptor is up-regulated in primary prostate cancer and commonly persists in metastatic disease. *Cancer Res* 2002; **62**: 2942–2950.
- Scorilas A, Plebani M, Mazza S, Basso D, Soosaipillai AR, Katsaros N *et al*. Serum human glandular kallikrein (hK2) and insulin-like growth factor 1 (IGF-1) improve the discrimination between prostate cancer and benign prostatic hyperplasia in combination with total and %free PSA. *Prostate* 2003; **54**: 220–229.
- Oliver SE, Barrass B, Gunnell DJ, Donovan JL, Peters TJ, Persad RA *et al*. Serum insulin-like growth factor-I is positively associated with serum prostate-specific antigen in middle-aged men without evidence of prostate cancer. *Cancer Epidemiol Biomarkers Prev* 2004; **13**: 163–165.
- Frasca F, Pandini G, Sciacca L, Pezzino V, Squatrito S, Belfiore A *et al*. The role of insulin receptors and IGF-I receptors in cancer and other diseases. *Arch Physiol Biochem* 2008; **114**: 23–37.
- Hellawell GO, Ferguson DJ, Brewster SF, Macaulay VM. Chemosensitization of human prostate cancer using antisense agents targeting the type 1 insulin-like growth factor receptor. *BJU Int* 2003; **91**: 271–277.
- Krueckl SL, Sikes RA, Edlund NM, Bell RH, Hurtado-Coll A, Fazli L *et al*. Increased insulin-like growth factor I receptor expression and signaling are components of androgen-independent progression in a lineage-derived prostate cancer progression model. *Cancer Res* 2004; **64**: 8620–8629.
- Nickerson T, Chang F, Lorimer D, Smeekens SP, Sawyers CL, Pollak M. *In vivo* progression of LAPC-9 and LNCaP prostate cancer models to androgen independence is associated with increased expression of insulin-like growth factor I (IGF-I) and IGF-I receptor (IGF-IR). *Cancer Res* 2001; **61**: 6276–6280.
- Huynh H, Seyam RM, Brock GB. Reduction of ventral prostate weight by finasteride is associated with suppression of insulin-like growth factor I (IGF-I) and IGF-I receptor genes and with an increase in IGF binding protein 3. *Cancer Res* 1998; **58**: 215–218.
- Pandini G, Mineo R, Frasca F, Roberts Jr CT, Marcelli M, Vigneri R *et al*. Androgens up-regulate the insulin-like growth factor-I receptor in prostate cancer cells. *Cancer Res* 2005; **65**: 1849–1857.
- Ohlsson C, Mohan S, Sjogren K, Tivesten A, Isgaard J, Isaksson O *et al*. The role of liver-derived insulin-like growth factor-I. *Endocr Rev* 2009; **30**: 494–535.
- Butler AA, Yakar S, Gewolb IH, Karas M, Okubo Y, LeRoith D. Insulin-like growth factor-I receptor signal transduction: at the interface between physiology and cell biology. *Comp Biochem Physiol B* 1998; **121**: 19–26.
- Thomas GV, Horvath S, Smith BL, Crosby K, Lebel LA, Schrage M *et al*. Antibody-based profiling of the phosphoinositide 3-kinase pathway in clinical prostate cancer. *Clin Cancer Res* 2004; **10**: 8351–8356.
- Muller M, Rink K, Krause H, Miller K. PTEN/MMAC1 mutations in prostate cancer. *Prostate Cancer Prostatic Dis* 2000; **3**(Suppl 1): S32.
- Trotman LC, Niki M, Dotan ZA, Koutcher JA, Di Cristofano A, Xiao A *et al*. Pten dose dictates cancer progression in the prostate. *PLoS Biol* 2003; **1**: 27.
- Takahara K, Tearle H, Ghaffari M, Gleave ME, Pollak M, Cox ME. Human prostate cancer xenografts in *lit/lit* mice exhibit reduced growth and androgen-independent progression. *Prostate* 2011; **71**: 525–537.
- Whang YE, Wu X, Suzuki H, Reiter RE, Tran C, Vessella RL *et al*. Inactivation of the tumor suppressor PTEN/MMAC1 in advanced human prostate cancer through loss of expression. *Proc Natl Acad Sci USA* 1998; **95**: 5246–5250.
- Yoshimoto M, Joshua AM, Cunha IW, Coudry RA, Fonseca FP, Ludkovski O *et al*. Absence of TMPRSS2:ERG fusions and PTEN losses in prostate cancer is associated with a favorable outcome. *Mod Pathol* 2008; **21**: 1451–1460.
- Wang S, Gao J, Lei Q, Rozengurt N, Pritchard C, Jiao J *et al*. Prostate-specific deletion of the murine Pten tumor suppressor gene leads to metastatic prostate cancer. *Cancer Cell* 2003; **4**: 209–221.
- Mulholland DJ, Tran LM, Li Y, Cai H, Morim A, Wang S *et al*. Cell autonomous role of PTEN in regulating castration-resistant prostate cancer growth. *Cancer Cell* 2011; **19**: 792–804.
- Suzuki A, Yamaguchi MT, Ohteki T, Sasaki T, Kaisho T, Kimura Y *et al*. T cell-specific loss of Pten leads to defects in central and peripheral tolerance. *Immunity* 2001; **14**: 523–534.
- Wu X, Wu J, Huang J, Powell WC, Zhang J, Matusik RJ *et al*. Generation of a prostate epithelial cell-specific Cre transgenic mouse model for tissue-specific gene ablation. *Mech Dev* 2001; **101**: 61–69.
- Godfrey P, Rahal JO, Beamer WG, Copeland NG, Jenkins NA, Mayo KE. GHRH receptor of little mice contains a missense mutation in the extracellular domain that disrupts receptor function. *Nat Genet* 1993; **4**: 227–232.
- Moussavi M, Fazli L, Tearle H, Guo Y, Cox M, Bell J *et al*. Oncolysis of prostate cancers induced by vesicular stomatitis virus in PTEN knockout mice. *Cancer Res* 2010; **70**: 1367–1376.

- 32 Luchman HA, Benediktsson H, Villemaire ML, Peterson AC, Jirik FR. The pace of prostatic intraepithelial neoplasia development is determined by the timing of Pten tumor suppressor gene excision. *PLoS One* 2008; **3**: 15.
- 33 Mulholland DJ, Kobayashi N, Ruscetti M, Zhi A, Tran LM, Huang J *et al.* Pten loss and RAS/MAPK activation cooperate to promote EMT and metastasis initiated from prostate cancer stem/progenitor cells. *Cancer Res* 2012; **72**: 1878–1889.
- 34 Majeed N, Blouin MJ, Kaplan-Lefko PJ, Barry-Shaw J, Greenberg NM, Gaudreau P *et al.* A germ line mutation that delays prostate cancer progression and prolongs survival in a murine prostate cancer model. *Oncogene* 2005; **24**: 4736–4740.
- 35 Furukawa J, Wraight CJ, Freier SM, Peralta E, Atley LM, Monia BP *et al.* Antisense oligonucleotide targeting of insulin-like growth factor-1 receptor (IGF-1R) in prostate cancer. *Prostate* 2010; **70**: 206–218.
- 36 Anzo M, Cobb LJ, Hwang DL, Mehta H, Said JW, Yakar S *et al.* Targeted deletion of hepatic Igf1 in TRAMP mice leads to dramatic alterations in the circulating insulin-like growth factor axis but does not reduce tumor progression. *Cancer Res* 2008; **68**: 3342–3349.
- 37 Szabolcs M, Keniry M, Simpson L, Reid LJ, Koujak S, Schiff SC *et al.* Irs2 inactivation suppresses tumor progression in Pten^{+/-} mice. *Am J Pathol* 2009; **174**: 276–286.
- 38 Schally AV, Varga JL. Antagonists of growth hormone-releasing hormone in oncology. *Comb Chem High Throughput Screen* 2006; **9**: 163–170.
- 39 Stangelberger A, Schally AV, Varga JL, Hammann BD, Groot K, Halmos G *et al.* Antagonists of growth hormone releasing hormone (GHRH) and of bombesin/gastrin releasing peptide (BN/GRP) suppress the expression of VEGF, bFGF, and receptors of the EGF/HER family in PC-3 and DU-145 human androgen-independent prostate cancers. *Prostate* 2005; **64**: 303–315.
- 40 Kong D, Banerjee S, Ahmad A, Li Y, Wang Z, Sethi S *et al.* Epithelial to mesenchymal transition is mechanistically linked with stem cell signatures in prostate cancer cells. *PLoS One* 2010; **5**: e12445.
- 41 van der Pluijm G. Epithelial plasticity, cancer stem cells and bone metastasis formation. *Bone* 2011; **48**: 37–43.